Automatica 140 (2022) 110213

Contents lists available at ScienceDirect

Automatica

journal homepage: www.elsevier.com/locate/automatica

Brief paper

Leak detection, size estimation and localization in branched pipe flows☆

Henrik Anfinsen, Ole Morten Aamo *

Department of Engineering Cybernetics, Norwegian University of Science and Technology (NTNU), 7491 Trondheim, Norway

ARTICLE INFO

Article history:
Received 12 June 2020
Received in revised form 24 September 2021
Accepted 6 January 2022
Available online 10 March 2022

Keywords:
Distributed parameter systems
Hyperbolic systems
Linear systems
Leak detection

ABSTRACT

We design a leak detection, size estimation and localization algorithm for a branched pipe system, requiring flow and pressure measurements to be taken at the inlet and outlet boundaries, only. By showing that the pipe system model can be mapped into a system of coupled, linear hyperbolic PDEs (partial differential equations), with the parametric uncertainties caused by the leak appearing in a particular way, established methods can be applied to obtain state and parameter estimates. Analyzing the structure of the parametric uncertainties that appear in the obtained adaptive observer canonical form, we prove that total leak size can be estimated regardless of how leaks are distributed in the pipe network. Moreover, any number of point leaks can be located, provided they occur sufficiently separated in time.

1. Introduction

Being able to accurately detect and find leaks in pipelines is important, not only to avoid the economical impact of losses, but also to protect the environment. Leaking oil and gas pipelines, for instance, may cause severe damage to the environment (Shivananju et al., 2013). Therefore, many methods for leak detection and localization exist today, for instance the use of distributed optical fiber sensing technology (Ren et al., 2018), the use of piezoceramic transducers (Zhu et al., 2017), ultrasound (Zhang, Huang, Zhao, Wang, & Wang, 2017), discretization and the use of Luenberger observer (Xie, Xu, & Dubljevic, 2019) and magnetic flux leakage detection (Feng, Li, Lu, Liu, & Ma, 2017). A recent, comprehensive overview of leak detection methods can be found in Adegboye, Fung, and Karnik (2019).

Leak detection methods are often divided into two main categories (Lang, Li, Cao, Li, & Ren, 2018): *internal monitoring methods*, and *external monitoring* methods. Internal methods encompass for instance ultrasound (Qidwai, 2009) and magnetic flux leakage detection (Feng et al., 2017). These are considered accurate, but may be easy to obstruct, require more expensive equipment, and may require distributed measurements along the pipe. External methods use field instrumentation, like for instance pressure, flow and temperature measurements (Timashev & Bushinskaya, 2016), which are often taken at pipe inlets and outlets, only. In Aamo (2016), a leak detection algorithm for a single pipe is proposed, that only requires measurements of pressure and volumetric flow at the inlet and outlet of the pipe. The algorithm simultaneously estimates the leak size and leak position in the pipe. The method is based on a distributed parameters model of the pipe obtained from mass and momentum conservations for a single phase fluid flow, which leads to a set of (linearized) hyperbolic partial differential equations (PDE). *Infinite-dimensional backstepping* is then used to design an observer estimating the uncertain parameters of the system.

The backstepping technique for estimation and control of distributed parameter systems has received a lot of attention in the last two decades. It appeared for the first time in Liu (2003), for the stabilization of an unstable parabolic PDE, and later in Krstić and Smyshlyaev (2008) for the stabilization of a scalar hyperbolic PDE. Extensions to gradually more involved hyperbolic PDEs followed in the milestone papers (Di Meglio, Vazquez, & Krstić, 2013; Hu, Di Meglio, Vazquez, & Krstić, 2016; Vazquez, Krstić, & Coron, 2011). Infinite-dimensional backstepping has the advantage of avoiding spatial discretization of the PDEs before an eventual implementation (late lumping), and also greatly facilitates adaptive schemes that can handle parametric uncertainties (Anfinsen & Aamo, 2019; Smyshlyaev & Krstić, 2010).

We will in this paper extend the result from Aamo (2016), expanding the leak detection method for a single pipe into a pipe system where a single pipe is branched into an arbitrary number of n pipes. The key approach now is to introduce a series of transformations that maps the considered system into a familiar form usually referred to as $n+m$ systems. A non-adaptive

☆ The material in this paper was not presented at any conference. This paper was recommended for publication in revised form by Associate Editor Rafael Vazquez under the direction of Editor Miroslav Krstic.

* Corresponding author.
E-mail addresses: henrik.anfinsen@ntnu.no (H. Anfinsen), aamo@ntnu.no (O.M. Aamo).

https://doi.org/10.1016/j.automatica.2022.110213

observer for this type of systems was designed in Hu et al. (2016), based on which an adaptive version was developed in Anfinsen and Aamo (2017).

The notation $\mathbb{1}_{n\times m}$ indicates an $n \times m$ matrix with all components set to 1. The notation I_n indicates an $n \times n$ identity matrix. The notation e_i indicates a vector of appropriate length with the value 1 at the i'th position, and zeros elsewhere. The partial derivative is usually denoted ∂_x to indicate differentiation with respect to the variable x.

2. Modeling and problem statement

The pipe flow is modeled as a standard hydraulic transmission line (see Egeland and Gravdahl (2002, Section 11.2.7)). Leaks are straightforwardly accommodated in the mass balance, while for the momentum balance, the derivations from Bajura (1971) are employed. The resulting model is

$$\partial_t p_i(z,t) + \frac{\bar{\beta}}{A_i}\partial_z q_i(z,t) = -\frac{\bar{\beta}}{A_i} d_i(z)\chi_i \tag{1a}$$

$$\partial_t q_i(z,t) + \frac{A_i}{\rho}\partial_z p_i(z,t) = -\frac{F_i}{\rho} q_i(z,t) - A_i g \sin(\phi_i(z)) - \frac{\eta_i}{A_i} d_i(z)\chi_i \tag{1b}$$

for $i = 0, 1, \dots, n$, defined for $t \geq 0$, $z \in [0, l_i]$, where p_i is the pressure, q_i is the volumetric flow for pipe i, $\bar{\beta}$ is the fluid's bulk modulus, ρ is the fluid's density, A_i is the cross sectional area of pipe segment i, F_i is the friction factor for pipe segment i, g is the gravity constant, and $\phi_i(z)$ is the inclination angle of pipe i. The factors χ_i and d_i are the leak size and distribution in pipe segment i. We assume the χ_i's are non-negative constants, and that the distributions d_i are nonnegative and normalized, that is

$$d_i(z) \geq 0, \forall z \in [0, l_i], \qquad i = 0, 1, \dots, n, \tag{2a}$$

$$\int_0^{l_i} d_i(z)dz = 1, \qquad i = 0, 1, \dots, n. \tag{2b}$$

The factors η_i are parameters which depend on the shape, size and direction of the leaks, and follow from the derivations in Bajura (1971). It is argued in Bajura (1971) that a good approximation of η_i can be taken as

$$\eta_i = \gamma_{i,d} q_{i,0} \tag{3}$$

where $q_{i,0}$ is the steady-state volumetric flow through pipe i, and $\gamma_{i,d} < 1$ is a factor that depends on the shape, size and direction of the leaks. For point leaks,

$$\gamma_{i,d} = 0.8 \tag{4}$$

is found experimentally (Bajura, 1971).

We assume that the $n+1$ pipe segments are branched in the sense that pipe $i = 0$ is connected to a source reservoir, and then branched into n individual pipes that supply n communities of consumers (see Fig. 1 for a sketch of the case $n = 3$). The coordinate systems for the pipes are defined such that the branching point is at $z = 0$ for every pipe. This means that the pressure must be the same in every pipe at $z = 0$, and the sum of flows at $z = 0$ must be zero. The conditions at the other end of the pipes ($z = l_i$) are governed by the reservoir pressure and consumer flows. This can be expressed by the following boundary conditions

$$p_0(l_0,t) = p_{0,l_0}(t), \qquad q_i(l_i,t) = q_{i,l_i}(t), \tag{5a}$$

$$q_0(0,t) = -\sum_{j=1}^{n} q_j(0,t), \qquad p_i(0,t) = p_0(0,t), \tag{5b}$$

for $i = 1, 2, \dots, n$, for a given reservoir pressure $p_{0,l_0}(t)$ and flows to consumers, $q_{i,l_i}(t)$ that may vary with time. In the case of an infinite reservoir, the pressure $p_{0,l_0}(t)$ may be taken as constant i.e. $p_{0,l_0}(t) = p_0$. The initial conditions are given as $p_i(z,t) = p_{i,0}(z)$, $q_i(z,t) = q_{i,0}(z)$, $z \in [0, l_i]$. Pressure and flow are measured at $z = l_i$ for all pipes, that is

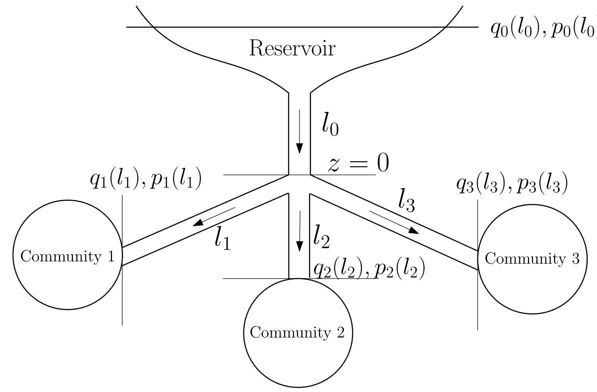

Fig. 1. Water supply system for $n = 3$.

$$q_l(t) = \begin{bmatrix} q_0(l_0,t) & q_1(l_1,t) & \dots & q_n(l_n,t) \end{bmatrix}^T \tag{6a}$$

$$p_l(t) = \begin{bmatrix} p_0(l_0,t) & p_1(l_1,t) & \dots & p_n(l_n,t) \end{bmatrix}^T \tag{6b}$$

are measured. No measurements are taken at the branching point $z = 0$, which is the main source of difficulty in this paper as compared to Aamo (2016).

3. Mapping to adaptive observer canonical form

The goal of this section is to rewrite the system consisting of (1) and (5) into the familiar form

$$u_t(x,t) + \Lambda u_x(x,t) = C_1(x)v(x,t) \tag{7a}$$

$$v_t(x,t) - \Lambda v_x(x,t) = C_2(x)u(x,t) \tag{7b}$$

$$u(0,t) = Q_0 v(0,t) + \kappa \tag{7c}$$

$$v(1,t) = R_1 u(1,t) + B_1 q_l(t) \tag{7d}$$

$$y(t) = u(1,t) \tag{7e}$$

for some functions $C_1, C_2 \in \mathcal{C}([0,1])^{(n+1)\times(n+1)}$, diagonal matrix $\Lambda \in \mathbb{R}^{(n+1)\times(n+1)}$, $\Lambda > 0$, matrices $Q_0, R_1, B_1 \in \mathbb{R}^{(n+1)\times(n+1)}$ and vector $\kappa \in \mathbb{R}^{n+1}$. The initial conditions are given as $u(x,0) = u_0(x)$, $v(x,0) = v_0(x)$ for $u_0, v_0 \in \mathcal{C}([0,1])^{n+1}$. The signal $q_l(t)$ is measured and defined in (6a). The signal y in (7e) can be considered measured, since it can be constructed from available measured signals. The desirable features of the form (7) are the diagonal Λ and the fact that the uncertain leak parameters appear at the boundary rather than in the interior domain, which is the case in (1). Several results from the literature (Anfinsen & Aamo, 2017; Hu et al., 2016; Hu, Vazquez, Meglio, & Krstić, 2019) apply to (7), and are employed for observer design in Section 4. The remainder of Section 3 provides the transformations bringing (1) into the form (7).

3.1. Characterizing the leak location

Firstly, we rewrite system (1) in a similar manner as was done in Aamo (2016). This is to better facilitate the transformation used for mapping system (1), (5) into system (7). Defining

$$\delta_i(z) = z - \int_0^z \int_\eta^{l_i} d_i(\gamma) d\gamma d\eta, \tag{8}$$

we have $\delta_i'(z) = 1 - \int_z^{l_i} d_i(\gamma)d\gamma$, $\delta_i''(z) = d_i(z)$ and the dynamics (1) can then be written

$$\partial_t p_i(z,t) + \frac{\bar{\beta}}{A_i}\partial_z q_i(z,t) = -\frac{\bar{\beta}}{A_i}\delta_i''(z)\chi_i \tag{9a}$$

$$\partial_t q_i(z,t) + \frac{A_i}{\rho}\partial_z p_i(z,t) = -\frac{F_i}{\rho}q_i(z,t) - A_i g\sin(\phi_i(z)) - \frac{\eta_i}{A_i}\delta_i''(z)\chi_i. \tag{9b}$$

Furthermore, we note that (8) satisfies

$$\delta_i(0) = \delta_i'(0) = 0, \qquad \delta_i'(l_i) = 1 \tag{10a}$$

$$\delta_i(l_i) = l_i - \nu_i, \qquad \nu_i = \int_0^{l_i}\int_\eta^{l_i} d_i(\gamma)d\gamma d\eta \tag{10b}$$

for all $i = 0, 1, 2, \dots, n$. The quantity ν_i relates in general to the spatial distribution of the leak, but gets a particular meaning in the case of a point leak.

Lemma 1. *Suppose pipe i has a single point leak located at $z = z^* \in [0, l_i]$. Then, $\nu_i = z^*$.*

Lemma 1 is a minor modification of Aamo (2016, Corollary 12), so the proof is omitted.

In a straightforward manner, Lemma 1 can be extended into the following corollary, which is an extension of Aamo (2016, Corollary 13) (therefore omitting the proof). It relates ν_i to the locations of multiple point leaks.

Corollary 2. *Suppose pipe i has m_i point leaks of sizes $\chi_{i,1}, \chi_{i,2}, \dots, \chi_{i,m_i}$, at locations $z = z_{i,j}^* \in [0, l_i]$, $j = 1, 2, \dots, m_i$. Then*

$$\nu_i = \frac{1}{\sum_{j=1}^{m_i}\chi_{i,j}}\sum_{j=1}^{m_i}\chi_{i,j}z_{i,j}^*. \tag{11}$$

3.2. Decoupling the convective terms

Consider the intermediate system

$$\bar{u}_t(x,t) + \Lambda\bar{u}_x(x,t) = C_1(x)\bar{v}(x,t) \tag{12a}$$

$$\bar{v}_t(x,t) - \Lambda\bar{v}_x(x,t) = C_2(x)\bar{u}(x,t) \tag{12b}$$

$$\bar{u}(0,t) = Q_0\bar{v}(0,t) \tag{12c}$$

$$\bar{v}(1,t) = R_1\bar{u}(1,t) + B_1 q_l(t) + B_1\chi \tag{12d}$$

$$y(t) = \bar{u}(1,t) - \theta \tag{12e}$$

for the system states

$$\bar{u}(x,t) = \begin{bmatrix}\bar{u}_0(x,t) & \bar{u}_1(x,t) & \dots & \bar{u}_n(x,t)\end{bmatrix}^T \tag{13a}$$

$$\bar{v}(x,t) = \begin{bmatrix}\bar{v}_0(x,t) & \bar{v}_1(x,t) & \dots & \bar{v}_n(x,t)\end{bmatrix}^T \tag{13b}$$

and where C_1, C_2, Q_0, R_1, B_1 are the same coefficients as in (7), $\theta \in \mathbb{R}^{n+1}$ is a vector of unknown coefficients, and

$$\chi = \begin{bmatrix}\chi_0 & \chi_1 & \dots & \chi_n\end{bmatrix}^T, \qquad \chi_i = \sum_{j=1}^{m_i}\chi_{i,j}, \tag{14}$$

is a vector of the individual pipes' total leak sizes. The initial conditions are given as $\bar{u}(x,0) = \bar{u}_0(x)$, $\bar{v}(x,0) = \bar{v}_0(x)$ for $\bar{u}_0, \bar{v}_0 \in \mathcal{C}([0,1])^{n+1}$.

Lemma 3. *The transformation*

$$\bar{u}_i(x,t) = \frac{1}{2}\Bigg(q_i(xl_i,t) + \delta_i'(xl_i)\chi_i + \frac{A_i}{\sqrt{\bar{\beta}\rho}}\Bigg(p_i(xl_i,t) + \rho g\int_0^{xl_i}\sin(\phi_i(\gamma))d\gamma + \frac{\rho}{A_i^2}\eta_i\delta_i'(xl_i)\chi_i - \frac{F_i}{A_i}\delta_i(xl_i)\chi_i\Bigg)\Bigg)e^{\gamma_i x} \tag{15a}$$

$$\bar{v}_i(x,t) = \frac{1}{2}\Bigg(q_i(xl_i,t) + \delta_i'(xl_i)\chi_i - \frac{A_i}{\sqrt{\bar{\beta}\rho}}\Bigg(p_i(xl_i,t) + \rho g\int_0^{xl_i}\sin(\phi_i(\gamma))d\gamma + \frac{\rho}{A_i^2}\eta_i\delta_i'(xl_i)\chi_i - \frac{F_i}{A_i}\delta_i(xl_i)\chi_i\Bigg)\Bigg)e^{-\gamma_i x} \tag{15b}$$

for $i = 0, 1, \dots, n$, maps the system consisting of (1) and (5) into (12), with coefficients

$$\Lambda = diag[\lambda], \qquad C_j(x) = diag[c_j(x)] \tag{16a}$$

$$Q_0 = I_{n+1} - \frac{2}{A_T}a\mathbb{1}_{1\times(n+1)} \tag{16b}$$

$$R_1 = -e^{-2\Gamma}, \qquad B_1 = e^{-\Gamma}, \tag{16c}$$

where

$$\lambda = \begin{bmatrix}\lambda_0 & \lambda_1 & \dots & \lambda_n\end{bmatrix}^T \tag{17a}$$

$$c_j(x) = \begin{bmatrix}c_{0,j}(x) & c_{1,j}(x) & \dots & c_{n,j}(x)\end{bmatrix}^T \tag{17b}$$

$$\theta = \begin{bmatrix}\theta_0 & \theta_1 & \dots & \theta_n\end{bmatrix}^T, \tag{17c}$$

$$\Gamma = diag[\gamma_0, \gamma_1, \dots, \gamma_n] \tag{17d}$$

for $j = 1, 2$, with elements

$$\lambda_i = \frac{1}{l_i}\sqrt{\frac{\bar{\beta}}{\rho}}, \qquad \gamma_i = \frac{l_i F_i}{2\sqrt{\bar{\beta}\rho}} \tag{18a}$$

$$c_{i,1}(x) = -\lambda_i\gamma_i e^{2\gamma_i x}, \qquad c_{i,2}(x) = -\lambda_i\gamma_i e^{-2\gamma_i x} \tag{18b}$$

$$\theta_i = e^{\gamma_i}\chi_i\left(\frac{1}{2} + \frac{\gamma_i}{l_i}(\nu_i - l_i) + \frac{\eta_i}{2A_i}\sqrt{\frac{\rho}{\beta}}\right) \tag{18c}$$

$$a = \begin{bmatrix}A_0 & A_1 & \dots & A_n\end{bmatrix}^T, \qquad A_T = \sum_{i=0}^n A_i, \tag{18d}$$

for $i = 0, 1, \dots, n$.

We see that θ contains components that are functions of the leak sizes χ_i and leak positions ν_i, as well as the leak hole parameters η_i. It is thus an uncertain factor.

Proof. The proof of the mapping of (1) into (12a)–(12b) required very minor modifications compared to Aamo (2016), and is therefore omitted. The boundary conditions, however, need extra consideration.

The mapping of the dynamics into the dynamics is very similar to the corresponding mapping in Aamo (2016), and therefore omitted.

Evaluating (15) at $x = 0$ and using (10a), we find

$$\bar{u}_i(0,t) = \frac{1}{2}\left(q_i(0,t) + \frac{A_i}{\sqrt{\bar{\beta}\rho}}p_i(0,t)\right) \tag{19a}$$

$$\bar{v}_i(0,t) = \frac{1}{2}\left(q_i(0,t) - \frac{A_i}{\sqrt{\bar{\beta}\rho}}p_i(0,t)\right) \tag{19b}$$

and hence

$$q_i(0,t) = \bar{u}_i(0,t) + \bar{v}_i(0,t) \tag{20a}$$

$$p_i(0,t) = \frac{\sqrt{\bar{\beta}\rho}}{A_i}(\bar{u}_i(0,t) - \bar{v}_i(0,t)) \tag{20b}$$

for $i = 0, 1, \dots, n$. Inserting (20) into (5b) gives

$$\sum_{i=0}^{n} \bar{u}_i(0,t) = -\sum_{i=0}^{n} \bar{v}_i(0,t) \tag{21a}$$

$$A_j\bar{u}_0(0,t) - A_0\bar{u}_j(0,t) = A_j\bar{v}_0(0,t) - A_0\bar{v}_j(0,t) \tag{21b}$$

for $j = 1, 2, \dots, n$. These equations can be written

$$(Q_0^0 + Q_0^1)\bar{u}(0,t) = (-Q_0^0 + Q_0^1)\bar{v}(0,t) \tag{22}$$

where

$$Q_0^0 = \begin{bmatrix} \mathbb{1}_{1\times(n+1)} \\ 0_{n\times(n+1)} \end{bmatrix}, \quad Q_0^1 = \begin{bmatrix} 0 & 0 & \dots & 0 \\ A_1 & -A_0 & \dots & 0 \\ \vdots & \vdots & \ddots & \vdots \\ A_n & 0 & \dots & -A_0 \end{bmatrix}. \tag{23}$$

It is straightforward to show that $\det(Q_0^0 + Q_0^1) = A_0^{n-1}A_T$, and hence $Q_0^0 + Q_0^1$ is invertible since $A_0, A_T > 0$, which then gives

$$\bar{u}(0,t) = Q_0\bar{v}(0,t) \tag{24}$$

for

$$Q_0 = (Q_0^0 + Q_0^1)^{-1}(-Q_0^0 + Q_0^1) \tag{25}$$

which, when written out, has the form (16b). Similarly as for $\det(Q_0^0+Q_0^1)$, it is straightforward to prove that $\det(-Q_0^0+Q_0^1) = -A_0^{n-1}A_T$, and hence $\det(Q_0) = -1$, independent of n. The matrix Q_0 is thus invertible. In fact, it turns out that Q_0 is an involutory matrix, meaning that $Q_0^{-1} = Q_0$.

Evaluating the transformation (15) at $x = 1$, yields

$$\bar{u}_i(1,t) = \frac{1}{2}\left(q_i(l_i,t) + \chi_i + \frac{A_i}{\sqrt{\beta\rho}}\left(p_i(l_i,t) + h_i + \frac{\rho}{A_i^2}\eta_i\chi_i - \frac{F_i}{A_i}\delta_i(l_i)\chi_i\right)\right)e^{\gamma_i} \tag{26a}$$

$$\bar{v}_i(1,t) = \frac{1}{2}\left(q_i(l_i,t) + \chi_i - \frac{A_i}{\sqrt{\beta\rho}}\left(p_i(l_i,t) + h_i + \frac{\rho}{A_i^2}\eta_i\chi_i - \frac{F_i}{A_i}\delta_i(l_i)\chi_i\right)\right)e^{-\gamma_i} \tag{26b}$$

where we inserted (10a) and defined

$$h_i = \rho g\int_0^{l_i} \sin(\phi_i(\gamma))d\gamma. \tag{27}$$

Solving for $q_i(l_i,t)$ gives

$$q_i(l_i,t) = e^{-\gamma_i}\bar{u}_i(1,t) + e^{\gamma_i}\bar{v}_i(1,t) - \chi_i, \tag{28}$$

and hence

$$\bar{v}_i(1,t) = -e^{-2\gamma_i}\bar{u}_i(1,t) + e^{-\gamma_i}q_{i,l_i}(t) + e^{-\gamma_i}\chi_i \tag{29}$$

for $i = 0, 1, 2, \dots, n$, which on vectorized form can be written (12d), with R_1 and B_1 defined in (16c), and where we recall the definition of q_l as stated in (6a), and the vector χ defined in (14). □

3.3. Affine transformation

Lastly, we introduce an affine transformation mapping (12) to (7).

Lemma 4. *The transformation*

$$u(x,t) = \bar{u}(x,t) - G_1(x)\theta - H_1(x)\chi \tag{30a}$$

$$v(x,t) = \bar{v}(x,t) - G_2(x)\theta - H_2(x)\chi \tag{30b}$$

where

$$G_1(x) = e^{-\Gamma(1-x)}, \qquad G_2(x) = -e^{-\Gamma(1+x)} \tag{31a}$$

$$H_1(x) = \Gamma e^{\Gamma x}(1-x) \tag{31b}$$

$$H_2(x) = e^{-\Gamma x}(I - \Gamma(1-x)) \tag{31c}$$

maps system (12) into (7), with κ given as

$$\kappa = \begin{bmatrix} \kappa_0 & \kappa_1 & \dots & \kappa_n \end{bmatrix}^T = \Sigma\theta + \Pi\chi \tag{32}$$

where

$$\Sigma = \{\sigma_{ij}\}_{i,j=0,1,\dots,n} = -(Q_0 + I_{n+1})B_1 \tag{33a}$$

$$\Pi = \{\pi_{ij}\}_{i,j=0,1,\dots,n} = Q_0(I_{n+1} - \Gamma) - \Gamma. \tag{33b}$$

Proof. Differentiating (30a) with respect to time and space, respectively, and inserting into (12a) gives

$$0 = u_t(x,t) + \Lambda u_x(x,t) - C_1(x)v(x,t) + \Big(\Lambda G_1'(x) - C_1(x)G_2(x)\Big)\theta + \Big(\Lambda H_1'(x) - C_1(x)H_2(x)\Big)\chi \tag{34a}$$

Using the fact that (31) satisfy $\Lambda G_1'(x) = C_1(x)G_2(x)$, $\Lambda G_2'(x) = -C_2(x)G_1'(x)$ we obtain the dynamics (7a). A similar derivation with (30a) and (12a), using $\Lambda H_1'(x) = C_1(x)H_2(x)$, $\Lambda H_2'(x) = -C_2(x)H_1'(x)$ gives (7b). Now inserting (30) into the boundary condition (12d) and the measurement (7e) gives

$$\bar{v}(1,t) = R_1u(1,t) + \Big(R_1G_1(1) - G_2(1)\Big)\theta + \Big(R_1H_1(1) - H_2(1) + B_1\Big)\chi + B_1q_l(t) \tag{35a}$$

$$y(t) = u(1,t) + \Big(G_1(1) - I\Big)\theta + H_1(1)\chi \tag{35b}$$

Using that G_1, G_2, H_1, H_2 as defined in (31) satisfies

$$G_1(1) = I, \qquad G_2(1) = R_1 = -e^{-2\Gamma} \tag{36a}$$

$$H_1(1) = 0, \qquad H_2(1) = B_1 = e^{-\Gamma}, \tag{36b}$$

we obtain (7c)–(7d) and (7e). Lastly, using (30), the boundary condition (7d) gives (7d), with

$$\kappa = \Big(Q_0G_2(0) - G_1(0)\Big)\theta + \Big(Q_0H_2(0) - H_1(0)\Big)\chi. \tag{37}$$

Evaluating (31) at $x = 0$ gives $G_1(0) = e^{-\Gamma} = B_1$, $G_2(0) = -e^{-\Gamma} = -B_1$, $H_1(0) = \Gamma$, $H_2(0) = I - \Gamma$. and substituting this into (37) gives (32)–(33). □

4. Observer design

The system (7) has a well-investigated form usually referred to as an "$n + m$-system" (Hu et al., 2016), where in our case, the n and m in "$n + m$" both equal $n + 1$. An observer estimating the states (u, v) in a system in form (7) for the case $\kappa = 0$ was first proposed in Hu et al. (2016) for the constant coefficients-case. A stabilizing controller was also proposed. The extension of the controller to spatially varying coefficients was done in Hu et al. (2019), while the extension of the observer to spatially varying coefficients was done in Wilhelmsen, Anfinsen, and Aamo (2019). The observer achieves finite-time convergence.

An observer estimating an additive term κ entering at the boundary at $x = 0$ was first proposed for coupled 2×2 systems in Aamo (2013), and later extended to $n + m$-systems in Anfinsen and Aamo (2017) for the case with constant coefficients. However, the extension to spatially varying coefficients is straightforward by combining the results in Anfinsen and Aamo (2017) and Hu et al. (2019). As in the observer designs in Anfinsen and Aamo (2017) and Hu et al. (2019), we require a specific ordering of the transport speeds λ_i, $i = 0, 1, \dots, n$, as stated in the following assumption.

Assumption 5. The transport speeds λ_i, $i = 0, 1, \dots, n$ are arranged in a non-decreasing order, that is

$$\lambda_0 \le \lambda_1 \le \lambda_2 \le \cdots \le \lambda_n. \tag{38}$$

This assumption is not restrictive, since this can always be achieved by a permutation of the elements of u.

4.1. Observer and its properties

Combining the results of Anfinsen and Aamo (2017) and Hu et al. (2019), we propose the observer

$$\hat{u}_t(x,t) + \Lambda \hat{u}_x(x,t) = C_1(x)\hat{v}(x,t) + K_1(x)(y(t) - \hat{u}(1,t)) \tag{39a}$$

$$\hat{v}_t(x,t) - \Lambda \hat{v}_x(x,t) = C_2(x)\hat{u}(x,t) \tag{39b}$$

$$+ K_2(x)(y(t) - \hat{u}(1,t)) \tag{39c}$$

$$\hat{u}(0,t) = Q_0 \hat{v}(0,t) + \hat{\kappa}(t) \tag{39d}$$

$$\hat{v}(1,t) = R_1 y(t) + B_1 q_l(t) \tag{39e}$$

with the adaptive law for κ

$$\dot{\hat{\kappa}}(t) = L(y(t) - \hat{u}(1,t)), \qquad \hat{\kappa}(0) = \hat{\kappa}_0 \tag{40}$$

where $\hat{\kappa}_0 \in \mathbb{R}^{n+1}$, and some initial conditions $\hat{u}(x,0) = \hat{u}_0(x)$, $\hat{v}(x,0) = \hat{v}_0(x)$, where $\hat{u}_0, \hat{v}_0 \in \mathcal{C}([0,1])^{n+1}$, . The quantities K_1, K_2 are injection gains and L is an adaptive gain, all to be designed.

Consider the quantities

$$\Omega^\alpha(x,\xi) = [\omega^\alpha_{ij}(x,\xi)]_{i,j=0,1,\dots,n} \tag{41a}$$

$$\Omega^\beta(x,\xi) = [\omega^\beta_{ij}(x,\xi)]_{i,j=0,1,\dots,n} \tag{41b}$$

given as the solution to the kernel equations

$$\Lambda \Omega^\alpha_x(x,\xi) + \Omega^\alpha_\xi(x,\xi)\Lambda = C_1(x)\Omega^\beta(x,\xi) \tag{42a}$$

$$-\Lambda \Omega^\beta_x(x,\xi) + \Omega^\beta_\xi(x,\xi)\Lambda = C_2(x)\Omega^\alpha(x,\xi) \tag{42b}$$

$$\Lambda \Omega^\alpha(x,x) - \Omega^\alpha(x,x)\Lambda = 0 \tag{42c}$$

$$\Lambda \Omega^\beta(x,x) + \Omega^\beta(x,x)\Lambda = C_2(x) \tag{42d}$$

$$\Omega^\alpha(0,\xi) - Q_0 \Omega^\beta(0,\xi) = M(\xi) \tag{42e}$$

$$\omega^\alpha_{ij}(x,1) = 0, \quad 0 \le j < i \le n \tag{42f}$$

where $M(\xi)$ is a strictly lower triangular matrix with components $m_{ij}(x)$, that is

$$M(x) = \{m_{ij}(x)\}_{i,j=0,1,\dots,n} = \begin{cases} 0 & \text{if } 0 \le j \le i \le n \\ m_{ij}(x) & \text{otherwise.} \end{cases} \tag{43}$$

Well-posedness of the PDE (42) is ensured by Hu et al. (2019, Theorem A.1) and Assumption 5.

Theorem 6. *Consider system (7), the observer (39) and update law (40). Select the output injection gains K_1 and K_2 as*

$$K_1(x) = \Omega^\alpha(x,1)\Lambda - \int_x^1 \Omega^\alpha(x,\xi)d\xi F^\alpha L - F^\alpha L \tag{44a}$$

$$K_2(x) = \Omega^\beta(x,1)\Lambda - \int_x^1 \Omega^\beta(x,\xi)d\xi F^\alpha L \tag{44b}$$

and the adaptive gain L so that LF^α is Hurwitz, where

$$F^\alpha = \left(I_{n+1} + \int_0^1 M(\xi)d\xi\right)^{-1}. \tag{45}$$

Then

$$\hat{\kappa} \to \kappa \tag{46a}$$

$$\hat{u}(x,\cdot) \to u(x,\cdot), \qquad \hat{v}(x,\cdot) \to v(x,\cdot), \qquad \forall x \in [0,1] \tag{46b}$$

exponentially fast, with a rate of convergence governed by the eigenvalues of LF^α, which can be arbitrarily placed by selection of L.

This theorem will be proved over the next subsections.

4.2. Error dynamics

Define the estimation errors $\tilde{u} = u - \hat{u}$, $\tilde{v} = v - \hat{v}$, $\tilde{\kappa} = \kappa - \hat{\kappa}$, for which we immediately obtain the dynamics

$$\tilde{u}_t(x,t) + \Lambda \tilde{u}_x(x,t) = C_1(x)\tilde{v}(x,t) - K_1(x)\tilde{u}(1,t) \tag{47a}$$

$$\tilde{v}_t(x,t) - \Lambda \tilde{v}_x(x,t) = C_2(x)\tilde{u}(x,t) - K_2(x)\tilde{u}(1,t) \tag{47b}$$

$$\tilde{u}(0,t) = Q_0 \tilde{v}(0,t) + \tilde{\kappa}(t) \tag{47c}$$

$$\tilde{v}(1,t) = 0 \tag{47d}$$

and

$$\dot{\tilde{\kappa}}(t) = L\tilde{u}(1,t) \tag{48}$$

where the initial conditions $\tilde{u}(x,0) = \hat{u}_0(x)$, $\tilde{v}(x,0) = \hat{v}_0(x)$, are given as $\tilde{u}_0 = u_0 - \hat{u}_0$, $\tilde{v}_0 = v_0 - \hat{v}_0$.

4.3. Decoupling by backstepping

We proceed by designing the injection gains K_1 and K_2, and the adaption gain L by performing a backstepping transformation design. Consider the target system

$$\alpha_t(x,t) + \Lambda \alpha_x(x,t) = C_1(x)\beta(x,t) + F^\alpha L\alpha(1,t) + \int_x^1 B^\alpha(x,\xi)\beta(\xi,t)d\xi \tag{49a}$$

$$\beta_t(x,t) - \Lambda \beta_x(x,t) = \int_x^1 B^\beta(x,\xi)\beta(\xi,t)d\xi \tag{49b}$$

$$\alpha(0,t) = Q_0\beta(0,t) - \int_0^1 M(\xi)\alpha(\xi,t)d\xi + \tilde{\kappa}(t) \tag{49c}$$

$$\beta(1,t) = 0 \tag{49d}$$

for some matrices B^α, B^β of appropriate sizes and initial conditions $\alpha(x,0) = \alpha_0(x)$, $\beta(x,0) = \beta_0(x)$. Consider also the adaptive law

$$\dot{\tilde{\kappa}}(t) = L\alpha(1,t). \tag{50}$$

Lemma 7. *The backstepping transformation*

$$\tilde{u}(x,t) = \alpha(x,t) + \int_x^1 \Omega^\alpha(x,\xi)\alpha(\xi,t)d\xi \tag{51a}$$

$$\tilde{v}(x,t) = \beta(x,t) + \int_x^1 \Omega^\beta(x,\xi)\alpha(\xi,t)d\xi \tag{51b}$$

with $(\Omega^\alpha, \Omega^\beta)$ *as the solution to* (42)*, maps system* (49) and (50) *into* (47) and (48) *with injection gains* (K_1, K_2) *given from* (44)*, provided* (B^α, B^β) *satisfy the integral equations*

$$B^\alpha(x,\xi) = -\Omega^\alpha(x,\xi)C_1(\xi) - \int_x^\xi \Omega^\alpha(x,s)B^\alpha(s,\xi)ds \tag{52a}$$

$$B^\beta(x,\xi) = -\Omega^\beta(x,\xi)C_1(\xi) - \int_x^\xi \Omega^\beta(x,s)B^\alpha(s,\xi)ds. \tag{52b}$$

The proof of Lemma 7 follows the same steps as the proof of Lemma 10 in Anfinsen and Aamo (2017), with minor modifications to accommodate the spatially varying coefficients C_1 and C_2. The proof is therefore omitted.

4.4. Affine transformation

From the structure of system (49), we have $\beta \equiv 0$ for $t \geq t_{\max}$ (see Anfinsen and Aamo (2019, p. 126)), where

$$t_{\max} = \max_{i=0,1,\dots,n} \lambda_i^{-1} = \lambda_0^{-1}, \tag{53}$$

and the system is reduced into

$$\alpha_t(x,t) + \Lambda\alpha_x(x,t) = F^\alpha L\alpha(1,t) \tag{54a}$$

$$\alpha(0,t) = -\int_0^1 M(\xi)\alpha(\xi,t)d\xi + \tilde{\kappa}(t) \tag{54b}$$

with $\alpha(x,0) = \alpha_0(x)$. Consider the target system

$$w_t(x,t) + \Lambda w_x(x,t) = 0 \tag{55a}$$

$$w(0,t) = -\int_0^1 M(\xi)w(\xi,t)d\xi \tag{55b}$$

with $w(x,0) = w_0(x)$, and adaptive law

$$\dot{\hat{\kappa}}(t) = LF^\alpha\tilde{\kappa}(t) + Lw(1,t). \tag{56}$$

Lemma 8. *The affine transformation*

$$\alpha(x,t) = w(x,t) + F^\alpha\tilde{\kappa}(t) \tag{57}$$

maps system (55)*, with* $w_0(x) = \alpha_0(x) - F^\alpha\tilde{\kappa}(0)$ *and the adaptive law* (56)*, into* (54) *with the adaptive law* (50)*.*

Proof. Differentiating (57) with respect to time and space, respectively, and inserting the update law (50), gives

$$w_t(x,t) = \alpha_t(x,t) - F^\alpha\dot{\hat{\kappa}}(t) = \alpha_t(x,t) - F^\alpha L\alpha(1,t) \tag{58a}$$

$$w_x(x,t) = \alpha_x(x,t). \tag{58b}$$

Inserting (58) into (55a), gives

$$0 = w_t(x,t) + \Lambda w_x(x,t) = \alpha_t(x,t) - F^\alpha L\alpha(1,t) + \Lambda\alpha_x(x,t) \tag{59}$$

hence, (54a) holds. Evaluating (57) at $x = 0$ and inserting the result and (57) into (55b) gives

$$\alpha(0,t) = -\int_0^1 M(\xi)w(\xi,t)d\xi + \left(I_{n+1} + \int_0^1 M(\xi)d\xi\right)F^\alpha\tilde{\kappa}(t). \tag{60}$$

Hence F^α chosen as (45) gives the boundary condition (54b). The initial condition w_0 is given trivially as (57) at $t = 0$. Finally, plugging the affine transformation (57) into the adaptive law (50), we obtain (56).

4.5. Proof of Theorem 6

Proof. Since solutions of systems in the form (7) are bounded by an exponential growth rate, and hence cannot diverge to infinity in finite time (Anfinsen & Aamo, 2019, Theorem 1.1), it suffices to consider solutions for $t \geq t_0$ for some t_0 to establish convergence properties. From the dynamics (55), valid for $t \geq \lambda_0^{-1}$, and the lower triangular form of M (recall (43)), it follows that $w \equiv 0$ for $t \geq t_0$, where

$$t_0 = t_{tot} + \lambda_0^{-1}, \qquad t_{tot} = \sum_{i=0}^n \lambda_i^{-1}, \tag{61}$$

and (56) is hence reduced to

$$\dot{\hat{\kappa}}(t) = LF^\alpha\tilde{\kappa}(t) \tag{62}$$

for $t \geq t_0$. Since L is chosen by design so that LF^α is Hurwitz, we will have $\tilde{\kappa} \to 0$ exponentially fast, and hence (46a) holds.

Since $\beta \equiv 0$ and $w \equiv 0$ for $t \geq t_0$, it follows from Lemmas 7 and 8 that

$$\tilde{u}(x,t) = \left(I_{n+1} + \int_x^1 \Omega^\alpha(x,\xi)d\xi\right)F^\alpha\tilde{\kappa}(t) \tag{63a}$$

$$\tilde{v}(x,t) = \int_x^1 \Omega^\beta(x,\xi)d\xi F^\alpha\tilde{\kappa}(t). \tag{63b}$$

for $t \geq t_0$. Since all coefficients $\Omega^\alpha, \Omega^\beta, F^\alpha$, are bounded, and $\tilde{\kappa} \to 0$ at an exponential rate, it follows that $\tilde{u}(x,\cdot), \tilde{v}(x,\cdot) \to 0$ at an exponential rate, and hence (46b) holds.

5. Estimation of leak size and position

We will here use the exponentially converging estimate $\hat{\kappa}$ from Theorem 6 to estimate the total leak size in the system, which is obtained regardless of how the leak is distributed in the network, and regardless of the values of the leak hole parameters $\eta_i, i = 0, 1, \dots, n$. Then, under the additional assumption that the leak is a point leak, we prove that $\hat{\kappa}$ also reveals which branch contains the leak along with its location.

5.1. Total leak size estimation

From Theorem 6 and the following lemma, it follows that $\mathbb{1}^T\hat{\kappa} \to -\sum_{i=0}^n \chi_i$ exponentially fast.

Lemma 9. *For* κ *defined in* (32)*, we have*

$$\mathbb{1}^T\kappa = -\sum_{i=0}^n \chi_i. \tag{64}$$

Proof. From the definitions of Σ and Π in (33), we have

$$\mathbb{1}^T\Sigma = -\mathbb{1}^T(Q_0 + I_{n+1})B_1 = -\mathbb{1}^T(2I_{n+1} - \frac{2}{A_T}a\mathbb{1}^T)B_1 = -(2\mathbb{1}^T - \frac{2}{A_T}\mathbb{1}^Ta\mathbb{1}^T)B_1 = -(2\mathbb{1}^T - \frac{2}{A_T}A_T\mathbb{1}^T)B_1 = 0 \tag{65}$$

and

$$\begin{aligned}\mathbb{1}^T\Pi e_i &= \mathbb{1}^T(Q_0(I_{n+1}-\Gamma)-\Gamma)e_i\\ &= \mathbb{1}^T((I_{n+1}-\frac{2}{A_T}a\mathbb{1}^T)(I_{n+1}-\Gamma)-\Gamma)e_i\\ &= ((\mathbb{1}^T-\frac{2}{A_T}\mathbb{1}^Ta\mathbb{1}^T)(I_{n+1}-\Gamma)-\mathbb{1}^T\Gamma)e_i\\ &= ((\mathbb{1}^T-2\mathbb{1}^T)(I_{n+1}-\Gamma)-\mathbb{1}^T\Gamma)e_i\\ &= -\mathbb{1}^T((I_{n+1}-\Gamma)+\mathbb{1}^T\Gamma)e_i = -1. \end{aligned} \tag{66}$$

Combining (65) and (66), we have

$$\mathbb{1}^T\kappa = \mathbb{1}^T\Sigma\theta + \mathbb{1}^T\Pi\chi = \mathbb{1}^T\Pi\sum_{i=0}^n e_i\chi_i = -\sum_{i=0}^n \chi_i. \quad \square \tag{67}$$

5.2. Leak localization

The vector κ defined in (32) contains $n+1$ components that are linear combinations of the total of $2n+2$ components of χ and θ, meaning that all components of θ and χ cannot be uniquely extracted from κ. This comes from the fact that it is impossible, in the chosen approach, to identify an arbitrary leak distribution in the network from boundary measurements only, as shown in Aamo (2016). However, the most likely leak event, namely that a single point leak occurs in one of the branches, can be handled. Moreover, we can handle multiple leak events provided they occur sufficiently separated in time to allow parameter convergence in between events. Subject to this requirement, it turns out that the branch that contains the leak can be identified in finite time, and the location within the branch can be estimated with exponential convergence.

Theorem 10. *Consider system (7) and the observer of Theorem 6. Suppose the leak sizes and distributions*

$$\bar\chi = \begin{bmatrix}\bar\chi_0 & \bar\chi_1 & \dots & \bar\chi_n\end{bmatrix}^T, \quad \bar\nu = \begin{bmatrix}\bar\nu_0 & \bar\nu_1 & \dots & \bar\nu_n\end{bmatrix}^T \tag{68}$$

are known, and let $\bar\theta_i$ and $\bar\kappa_i$ denote the respective values obtained by (18c) and (32). *Suppose an additional point leak of size $\check\chi > 0$ occurs in pipe $k \in \{0, 1, \dots, n\}$ at location $z^* \in (0, l_k)$, and let θ and κ denote the (unknown) values obtained from* (32) and (18c), *respectively, after the occurrence of the new point leak. Let*

$$\hat{\check\chi}(t) = -\mathbb{1}^T\hat{\check\kappa}(t) \tag{69a}$$

$$\hat{\check\theta}_j(t) = \begin{bmatrix}\hat{\check\theta}_j^0(t) & \hat{\check\theta}_j^1(t) & \dots & \hat{\check\theta}_j^n(t)\end{bmatrix}^T \tag{69b}$$

$$\hat{\check\theta}_j^i(t) = \frac{\hat{\check\kappa}_i(t)-\pi_{ij}\hat{\check\chi}(t)}{\sigma_{ij}}, \quad i,j = 0, 1, \dots, n, \tag{69c}$$

$$\hat k(t) = \arg\min_{j\in\{0,1,\dots,n\}}\left|\hat{\check\theta}_j(t) - \mathbb{1}|\hat{\check\theta}_j(t)|\right| \tag{69d}$$

$$\hat\theta_k(t) = \bar\theta_k + \frac{1}{n+1}\mathbb{1}^T\hat{\check\theta}_k(t) \tag{69e}$$

$$\hat\chi_k(t) = \bar\chi_k + \hat{\check\chi}(t) \tag{69f}$$

$$\hat\nu_k(t) = l_k - \frac{\rho}{F_kA_k}\eta_k - \frac{l_k}{\gamma_k}\left(\frac{1}{2} - e^{-\gamma_k}\frac{\hat\theta_k(t)}{\hat\chi_k(t)}\right) \tag{69g}$$

$$\hat z^*(t) = \frac{1}{\hat{\check\chi}(t)}\left(\hat\chi_k(t)\hat\nu_k(t) - \bar\chi_k\bar\nu_k\right) \tag{69h}$$

where $\hat{\check\kappa}$ is generated from $\hat\kappa$ produced by Theorem 6 as

$$\hat{\check\kappa}(t) = \hat\kappa(t) - \bar\kappa. \tag{70}$$

Then, $\hat{\check\chi} \to \check\chi$ with exponential convergence. Moreover, there exists $T > 0$ after which $\hat k = k$, and $\hat z^* \to z^*$ with exponential convergence.

Remark 11. Notice that (69g) implicitly expresses in mathematical terms some properties that can be argued from intuition. (1) Division by $\hat{\check\chi}(t)$: clearly, localization requires that there actually is a leak in the network. (2) Division by F_k: localization requires viscous friction.

Remark 12. Note that in the case of multiple leaks present in pipe k prior to the new leak occurring, the positions of these leaks need not to be known for the new leak's position to be identified. Only the weighted sum $\bar\nu_k$ need to be known, which does not necessarily include the leaks' exact positions.

Proof. By Lemma 9, we have $\mathbb{1}^T\bar\kappa = -\sum_{i=0}^n\bar\chi_i$ and $\mathbb{1}^T\kappa = -\sum_{i=0}^n\bar\chi_i - \chi_k = \mathbb{1}^T\bar\kappa - \check\chi$, meaning that $\check\chi = -\mathbb{1}^T(\kappa-\bar\kappa) = -\mathbb{1}^T\check\kappa$ where we have defined

$$\check\kappa = \kappa - \bar\kappa. \tag{71}$$

Now, since by Theorem 6, $\hat\kappa \to \kappa$, and $\bar\kappa$ is assumed known, (69a) follows with $\hat{\check\kappa}$ generated using (70).

By the definition of κ in (32), we have before the occurrence of the new leak the following relationship

$$\bar\kappa_i = \sum_{j=0}^n\sigma_{ij}\bar\theta_j + \sum_{j=0}^n\pi_{ij}\bar\chi_j. \tag{72}$$

With the occurrence of the new leak, the expression for κ_i is

$$\kappa_i = \sum_{j=0}^n\sigma_{ij}\theta_j + \sum_{j=0}^n\pi_{ij}\chi_j. \tag{73}$$

Since $\chi_j = \bar\chi_j$, and $\theta_j = \bar\theta_j$ for all $j \neq k$, with $\chi_k = \bar\chi_k + \check\chi$, we have

$$\begin{aligned}\kappa_i &= \sum_{j=0}^n\sigma_{ij}\bar\theta_j + \sum_{j=0}^n\pi_{ij}\bar\chi_j + \sigma_{ik}(\theta_k-\bar\theta_k) + \pi_{ik}\check\chi\\ &= \bar\kappa_i + \sigma_{ik}\check\theta_k + \pi_{ik}\check\chi\end{aligned} \tag{74}$$

where we have defined

$$\check\theta_k = \theta_k - \bar\theta_k. \tag{75}$$

Likewise, we form $\check\kappa_i$ as the difference between the values of κ_i and $\bar\kappa_i$, which is found from (74) as

$$\check\kappa_i = \kappa_i - \bar\kappa_i = \sigma_{ik}\check\theta_k + \pi_{ik}\check\chi. \tag{76}$$

Written out, the components σ_{ij} and π_{ij} are

$$\sigma_{ij} = 2\frac{A_i}{A_T}e^{-\gamma_j} - 2\delta_{ij}e^{-\gamma_j} \tag{77a}$$

$$\pi_{ij} = \delta_{ij}(1-2\gamma_j) - 2\frac{A_i}{A_T}(1-\gamma_j) \tag{77b}$$

where

$$\delta_{ij} = \begin{cases}1 & \text{for } i=j\\ 0 & \text{otherwise.}\end{cases} \tag{78}$$

Assuming the leak is in pipe j, and based on (76), we let

$$\check\kappa_i = \sigma_{ij}\check\theta_j^i + \pi_{ij}\check\chi, \tag{79}$$

from which we obtain $n+1$ values of $\check\theta_j$ as

$$\check\theta_j^i = \frac{\check\kappa_i - \pi_{ij}\check\chi}{\sigma_{ij}}. \tag{80}$$

Consider the difference

$$\check{\theta}_j^i - \check{\theta}_j^m = \frac{\check{\kappa}_i - \pi_{ij}\check{\chi}}{\sigma_{ij}} - \frac{\check{\kappa}_m - \pi_{mj}\check{\chi}}{\sigma_{mj}} = \frac{\sigma_{ik}\check{\theta}_k + \pi_{ik}\check{\chi} - \pi_{ij}\check{\chi}}{\sigma_{ij}} - \frac{\sigma_{mk}\check{\theta}_k - \pi_{mk}\check{\chi} + \pi_{mj}\check{\chi}}{\sigma_{mj}} = \left(\frac{\sigma_{ik}}{\sigma_{ij}} - \frac{\sigma_{mk}}{\sigma_{mj}}\right)\check{\theta}_k + \left(\frac{\pi_{ik} - \pi_{ij}}{\sigma_{ij}} - \frac{\pi_{mk} - \pi_{mj}}{\sigma_{mj}}\right)\check{\chi} \quad (81)$$

where we have inserted (76) for $\check{\kappa}_i$. Clearly, when $j = k$, we have $\check{\theta}_j^i = \check{\theta}_j^m$ for all i, m, meaning that all $\check{\theta}_k^i$, $i = 0, 1, 2, \ldots n$, are equal. Consider now the case $j \neq k$, and $m = k$, $i \neq j$, $i \neq k$. Inserting the definitions (77), we get

$$\check{\theta}_j^i - \check{\theta}_j^m = \left(\frac{\sigma_{ik}}{\sigma_{ij}} - \frac{\sigma_{kk}}{\sigma_{kj}}\right)\check{\theta}_k + \left(\frac{\pi_{ik} - \pi_{ij}}{\sigma_{ij}} - \frac{\pi_{kk} - \pi_{kj}}{\sigma_{kj}}\right)\check{\chi}$$
$$= \left(\frac{2\frac{A_i}{A_T}e^{-\gamma_k}}{2\frac{A_i}{A_T}e^{-\gamma_j}} - \frac{2\frac{A_k}{A_T}e^{-\gamma_k} - 2e^{-\gamma_k}}{2\frac{A_k}{A_T}e^{-\gamma_j}}\right)\check{\theta}_k + \left(\frac{-2\frac{A_i}{A_T}(1-\gamma_k) + 2\frac{A_i}{A_T}(1-\gamma_j)}{2\frac{A_i}{A_T}e^{-\gamma_j}} - \frac{(1-2\gamma_k) - 2\frac{A_k}{A_T}(1-\gamma_k) + 2\frac{A_k}{A_T}(1-\gamma_j)}{2\frac{A_k}{A_T}e^{-\gamma_j}}\right)\check{\chi}$$
$$= \left(e^{\gamma_j - \gamma_k} - \frac{A_k - A_T}{A_k}e^{\gamma_j - \gamma_k}\right)\check{\theta}_k + \left((\gamma_k - \gamma_j)e^{\gamma_j} - \frac{A_T(1-2\gamma_k)}{2A_k e^{-\gamma_j}} - (\gamma_k - \gamma_j)e^{\gamma_j}\right)\check{\chi}$$
$$= \frac{A_T}{A_k}e^{\gamma_j - \gamma_k}\check{\theta}_k - \frac{1}{2}\frac{A_T}{A_k}(1 - 2\gamma_k)e^{\gamma_j}\check{\chi}. \quad (82)$$

For $\check{\theta}_k$, we have from the definitions (75) and (18c)

$$\check{\theta}_k = \theta_k - \bar{\theta}_k e^{\gamma_k}\chi_k\left(\frac{1}{2} + \frac{\gamma_k}{l_k}(\nu_k - l_k) + \frac{\eta_k}{2A_k}\sqrt{\frac{\rho}{\bar{\beta}}}\right) - e^{\gamma_k}\bar{\chi}_k\left(\frac{1}{2} + \frac{\gamma_k}{l_k}(\bar{\nu}_k - l_k) + \frac{\eta_k}{2A_k}\sqrt{\frac{\rho}{\bar{\beta}}}\right). \quad (83)$$

Utilizing that $\chi_k = \bar{\chi}_k + \check{\chi}$, this can be written

$$\check{\theta}_k = e^{\gamma_k}\frac{\gamma_k}{l_k}(\chi_k\nu_k - \bar{\chi}_k\bar{\nu}_k) + e^{\gamma_k}\check{\chi}\left(\frac{1}{2} - \gamma_k + \frac{\eta_k}{2A_k}\sqrt{\frac{\rho}{\bar{\beta}}}\right). \quad (84)$$

Inserting (84) into (82) gives

$$\check{\theta}_j^i - \check{\theta}_j^m = \frac{A_T}{A_k}\frac{\gamma_k}{l_k}e^{\gamma_j}(\chi_k\nu_k - \bar{\chi}_k\bar{\nu}_k) + \frac{1}{2}\frac{A_T}{A_k^2}e^{\gamma_j}\check{\chi}\eta_k\sqrt{\frac{\rho}{\bar{\beta}}}. \quad (85)$$

Recall that $\chi_k = \bar{\chi}_k + \check{\chi}$, and by Corollary 2,

$$\nu_k = \frac{1}{\chi_k}(\bar{\chi}_k\bar{\nu}_k + \check{\chi}z^*). \quad (86)$$

Inserting (86) into (85) gives

$$\check{\theta}_j^i - \check{\theta}_j^m = \frac{A_T}{A_k}e^{\gamma_j}\check{\chi}\left(\frac{\gamma_k}{l_k}z^* + \frac{1}{2}\frac{\eta_k}{A_k}\sqrt{\frac{\rho}{\bar{\beta}}}\right) > 0. \quad (87)$$

Hence, $\check{\theta}_j^i$ and $\check{\theta}_j^m$ are not equal for all $i \in \{0, 1, \ldots, n\}$ when $j \neq k$. As $t \to \infty$, by Theorem 6 $\hat{\kappa} \to \kappa$ exponentially, so $\left|\hat{\underline{\theta}}_j(t) - \mathbb{1}|\hat{\underline{\theta}}_j(t)|\right|$ converges exponentially to 0 if $j = k$, while to some number bounded away from zero if $j \neq k$. Hence, there exists $T > 0$ so that for $j \neq k$, $|\hat{\underline{\theta}}_k(t) - \mathbb{1}|\hat{\underline{\theta}}_k(t)\| < |\hat{\underline{\theta}}_j(t) - \mathbb{1}|\hat{\underline{\theta}}_j(t)\|$ for all $t > T$, and hence (69d) will result in $\hat{k} = k$ for $t > T$.

Solving (18c) for $i = k$ with respect to ν_k, and (86) with respect to z^* we have

$$\nu_k = l_k - \frac{l_k}{\gamma_k}\left(\frac{1}{2} - e^{-\gamma_k}\frac{\theta_k}{\chi_k}\right) - \frac{\rho}{F_k A_k}\eta_k \quad (88a)$$

$$z^* = \frac{1}{\check{\chi}}(\chi_k\nu_k - \bar{\chi}_k\bar{\nu}_k) \quad (88b)$$

where $\theta_k = \bar{\theta}_k + \check{\theta}_k$, $\chi_k = \bar{\chi}_k + \check{\chi}$ and where we have used the definition of γ_i in (18a). Substituting $\check{\chi}$ with its estimate $\hat{\check{\chi}}$, and $\check{\theta}_k$ with an average of the estimates of the components in the vector $\hat{\underline{\theta}}_k$, we obtain (69e)–(69h). □

6. Simulations

System (1) with boundary conditions (5) was implemented in MATLAB for a water supply system supplying water for two communities of consumers, that is $n = 2$. The following system parameters were used

$$\rho = 1000 \text{ kg/m}^2, \qquad \bar{\beta} = 2.15 \cdot 10^9 \text{ Pa}, \quad (89a)$$
$$A_0 = \frac{\pi}{4}(0.7)^2 \text{ m}^2, \qquad A_1 = A_2 = \frac{\pi}{4}(0.3)^2 \text{ m}^2 \quad (89b)$$
$$l_0 = 15 \text{ km}, \qquad l_1 = 12 \text{ km} \quad (89c)$$
$$l_2 = 10 \text{ km}, \qquad g = 9.81 \text{ m/s}^2, \quad (89d)$$

where we note that Assumption 5 is satisfied. The coefficients η_i, $i = 0, 1, 2$ are chosen according to (3) with $\gamma_{d,i} = 0.8$, $i = 0, 1, 2$, as suggested in Bajura (1971) for point leaks. The communities are assumed to have 50 and 70 thousand consumers, respectively, consuming an average of 150 L of water each per day. In addition, small fluctuations from this average are implemented as uniformly distributed white noise. The reservoir inlet is assumed to provide the required amount of water, with a boundary condition (5a) given from a constant atmospheric pressure, that is

$$p_0(l_0, t) = 10^5 \text{ Pa} \quad (90)$$

for all $t \geq 0$. The inclination angles ϕ_i are set to 0 for pipes 1 and 2, and so that the total vertical drop is 120 m for pipe 0. Plugging the parameters into the online pressure drop calculator (PipeLife, 2020), the friction factors were computed to be

$$\begin{bmatrix} F_0 & F_1 & F_2 \end{bmatrix} = \begin{bmatrix} 4.45 & 23.07 & 31.51 \end{bmatrix} \text{ kg/m}^3\text{s}. \quad (91)$$

The observer of Theorem 6 and position estimator of Theorem 10 were implemented in MATLAB, with all initial conditions set to zero. The matrix L is chosen so that the poles of the matrix LF^α are located at $(-1, -1 \pm 1j)$. Initially, there were no leaks in the system, with the following leaks occurring sequentially:

- $t = 50$ s: 10 L/s leak at $z = 1.2$ km in pipe $i = 0$.
- $t = 100$ s: 20 L/s leak at $z = 2.4$ km in pipe $i = 1$.
- $t = 150$ s: 10 /s leak at $z = 7.2$ km in pipe $i = 1$.

The spacing in time between the leaks is sufficient for the observer to converge before the occurrence of the next leak, as the simulation results in Figs. 2–5 show.

In Fig. 2, the flow in and out of the pipes at the in/outlets at $z = l_i$ are shown. A slight increase in the inflow of pipe $i = 0$ can be observed as the total leak size increases. In Fig. 3, the estimated leak sizes are shown. The leak sizes are correctly estimated approximately fifteen seconds after the occurrence of the leaks. Fig. 4 shows the estimated leak pipe index $\hat{k}$ for the three leaks, while Fig. 5 shows the estimated leak position for the three leaks. The converge times are approximately the same as for the estimated leak sizes: 15 s.

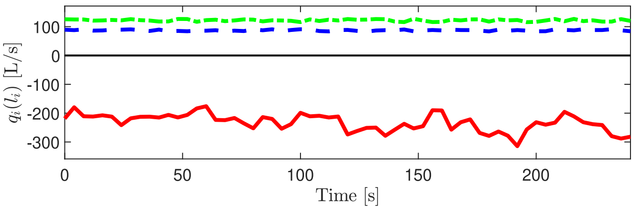

Fig. 2. Flow at the in and outlets for first (solid red), second (dashed blue) and third (dashed–dotted green) pipe.

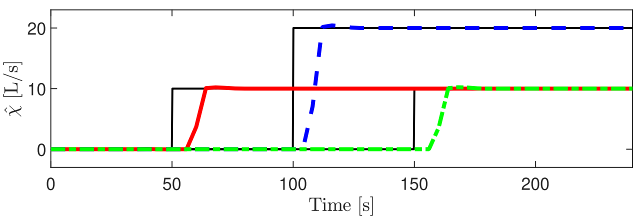

Fig. 3. Estimated leak size for first (solid red), second (dashed blue) and third (dashed–dotted green) leak.

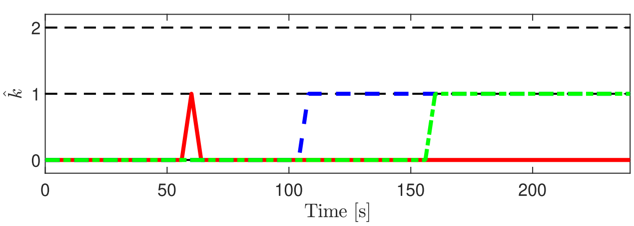

Fig. 4. Estimated leak pipe index for first (solid red), second (dashed blue) and third (dashed–dotted green) leak.

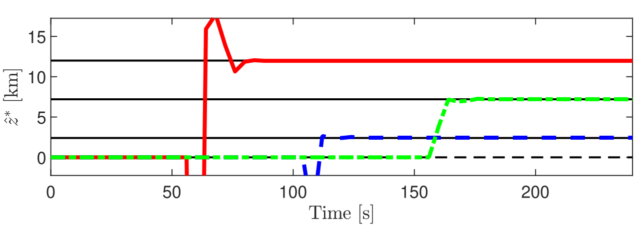

Fig. 5. Estimated leak position for first (solid red), second (dashed blue) and third (dashed–dotted green) leak.

7. Conclusions

We have extended the leak detection and localization algorithm from Aamo (2016) to also cover branched pipe systems with an arbitrary number of pipes, and multiple leaks. Subject to the assumption that leaks occur with sufficient spacing in time, the proposed method manages to correctly estimate the size, and position of each individual leak. Simulations show that the proposed observer manages to correctly estimate the leak sizes, identify the leaking pipes, and also estimate the leak positions in the pipes. Clearly, the simulations presented benefit from ideal conditions with perfectly known parameters. In practice, model structure errors, parametric uncertainty, particularly in friction factors, and sensing quality will affect the estimation accuracy. Experimental tests would give valuable insight into the practical feasibility of the approach.

Acknowledgment

The authors wish to thank Dr. Haavard Holta for valuable discussions.

References

Aamo, Ole Morten (2013). Disturbance rejection in 2 × 2 linear hyperbolic systems. *IEEE Transactions on Automatic Control*, *58*(5), 1095–1106.

Aamo, Ole Morten (2016). Leak detection, size estimation and localization in pipe flows. *IEEE Transactions on Automatic Control*, *61*(1), 246–251.

Adegboye, Mutiu Adesina, Fung, Wai-Keung, & Karnik, Aditya (2019). Recent advances in pipeline monitoring and oil leakage detection technologies: Principles and approaches. *Sensors*.

Anfinsen, Henrik, & Aamo, Ole Morten (2017). Disturbance rejection in general heterodirectional 1-D linear hyperbolic systems using collocated sensing and control. *Automatica*, *76*, 230–242.

Anfinsen, Henrik, & Aamo, Ole Morten (2019). *Adaptive control of hyperbolic pdes*. Springer International Publishing.

Bajura, Richard A. (1971). A model for flow distribution in manifolds. *Journal of Engineering for Gas Turbines and Power*, 7–12.

Di Meglio, Florent, Vazquez, Rafael, & Krstić, Miroslav (2013). Stabilization of a system of $n + 1$ coupled first-order hyperbolic linear PDEs with a single boundary input. *IEEE Transactions on Automatic Control*, *58*(12), 3097–3111.

Egeland, Olav, & Gravdahl, Jan Tommy (2002). Modeling and simulation for automatic control.

Feng, Jian, Li, Fangming, Lu, Senxiang, Liu, Jinhai, & Ma, Dazhong (2017). Injurious or noninjurious defect identification from MFL images in pipeline inspection using convolutional neural network. *IEEE Transactions on Instrumentation and Measurement*, *66*(7).

Hu, Long, Di Meglio, Florent, Vazquez, Rafael, & Krstić, Miroslav (2016). Control of homodirectional and general heterodirectional linear coupled hyperbolic PDEs. *IEEE Transactions on Automatic Control*, *61*(11), 3301–3314.

Hu, Long, Vazquez, Rafael, Meglio, Florent Di, & Krstić, Miroslav (2019). Boundary exponential stabilization of 1-d inhomogeneous quasilinear hyperbolic systems. *SIAM Journal on Control and Optimization*.

Krstić, Miroslav, & Smyshlyaev, Andrey (2008). Backstepping boundary control for first-order hyperbolic PDEs and application to systems with actuator and sensor delays. *Systems & Control Letters*, *57*(9), 750–758.

Lang, Xianming, Li, Ping, Cao, Jiangtao, Li, Yan, & Ren, Hong (2018). A small leak localization method for oil pipelines based on information fusion. *IEEE Sensors Journal*, *18*(15).

Liu, Weijiu (2003). Boundary feedback stabilization of an unstable heat equation. *SIAM Journal on Control and Optimization*, *42*, 1033–1043.

PipeLife (2020). Colebrook-white. https://tools.pipelife.com/Colebrook.

Qidwai, Uvais A. (2009). Autonomous corrosion detection in gas pipelines: A hybrid-fuzzy classifier approach using ultrasonic nondestructive evaluation protocols. *IEEE Transactions on Ultrasonics, Ferroelectrics and Frequency Control*, *56*(12), 2650–2665.

Ren, Liang, Jiang, Tao, guang Ji, Zi, sheng Lia, Dong, lin Yuan, Chao, & nan Li, Hong (2018). Pipeline corrosion and leakage monitoring based on the distributed optical fiber sensing technology. *Measurement*, 57–65.

Shivananju, B. N., Kiran, M., Nithin, S. P., Vidya, M. J., Hegde, G. M., & Asokan, S. (2013). Real time monitoring of petroleum leakage detection using etched fiber bragg grating. In *SPIE: Optics in precision engineering and nanotechnology, Vol. 8769*. Singapore.

Smyshlyaev, Andrey, & Krstić, Miroslav (2010). *Adaptive control of parabolic pdes*. Princeton University Press.

Timashev, Sviatoslav, & Bushinskaya, Anna (2016). Diagnostics and reliability of pipeline systems.

Vazquez, Rafael, Krstić, Miroslav, & Coron, Jean-Michel (2011). Backstepping boundary stabilization and state estimation of a 2 × 2 linear hyperbolic system. In *Decision and control and european control conference (CDC-ECC), 2011 50th IEEE conference on* (pp. 4937–4942).

Wilhelmsen, Nils Christian Aars, Anfinsen, Henrik, & Aamo, Ole Morten (2019). Minimum time bilateral observer design for 2 × 2 linear hyperbolic systems. In *European control conference 2019*. Naples, Italy.

Xie, Junyao, Xu, Xiaodong, & Dubljevic, Stevan (2019). Long range pipeline leak detection and localization using discrete observer and support vector machine. *Sustainable Energy: Process Systems Engineering*, *65*(7).

Zhang, Yua, Huang, Songlinga, Zhao, Weia, Wang, Shena, & Wang, Qing (2017). Electromagnetic ultrasonic guided wave long-term monitoring and data difference adaptive extraction method for buried oil-gas pipelines. *International Journal of Applied Electromagnetics and Mechanics*, *54*(3), 329–339.

Zhu, Junxiao, Ho, Siu Chun Michael, Patil, Devendra, Wang, Ning, Hirsch, Rachel, & Song, Gangbing (2017). Underwater pipeline impact localization using piezoceramic transducers. *Smart Materials and Structures*, *26*.

Henrik Anfinsen received his M.Sc. and Ph.D. degrees from the Department of Engineering Cybernetics at the Norwegian University of Science and Technology (NTNU) in 2013 and 2018, respectively. From 2018 to 2021, he worked at NTNU as a researcher. He is a co-author of the book Adaptive Control of Hyperbolic PDEs (Springer, 2019).

Ole Morten Aamo received the M.Sc. and Ph.D. degrees in engineering cybernetics from the Norwegian University of Science and Technology (NTNU), Trondheim, Norway, in 1992 and 2002, respectively. He is currently a professor with NTNU. His research interests include control of distributed parameter systems with special emphasis on control of fluid flows. He is a co-author of the books Flow Control by Feedback (Springer, 2003) and Adaptive Control of Hyperbolic PDEs (Springer, 2019).